

New determination of the adiabatic ionization potential of the BaOH radical from laser photoionization-molecular beam experiments and ab initio calculations

Maximiliano Rossa, Iván Cabanillas-Vidosa, Gustavo A. Pino, and Juan C. Ferrero

Citation: *J. Chem. Phys.* **136**, 064303 (2012); doi: 10.1063/1.3682283

View online: <http://dx.doi.org/10.1063/1.3682283>

View Table of Contents: <http://jcp.aip.org/resource/1/JCPSA6/v136/i6>

Published by the American Institute of Physics.

Related Articles

Ultrafast resonance-enhanced multiphoton ionization in the azabenzenes: Pyridine, pyridazine, pyrimidine, and pyrazine

J. Chem. Phys. **136**, 054309 (2012)

Angle-resolved metastable fragment yields spectra of N₂ and CO in K-edge excitation energy region

J. Chem. Phys. **136**, 054201 (2012)

Dissociative photoionization of methyl chloride studied with threshold photoelectron-photoion coincidence velocity imaging

J. Chem. Phys. **136**, 034304 (2012)

Communication: Manipulating the singlet-triplet equilibrium in organic biradical materials

JCP: BioChem. Phys. **5**, 12B401 (2011)

Communication: Manipulating the singlet-triplet equilibrium in organic biradical materials

J. Chem. Phys. **135**, 241101 (2011)

Additional information on J. Chem. Phys.

Journal Homepage: <http://jcp.aip.org/>

Journal Information: http://jcp.aip.org/about/about_the_journal

Top downloads: http://jcp.aip.org/features/most_downloaded

Information for Authors: <http://jcp.aip.org/authors>

ADVERTISEMENT

AIPAdvances

Submit Now

**Explore AIP's new
open-access journal**

- **Article-level metrics
now available**
- **Join the conversation!
Rate & comment on articles**

New determination of the adiabatic ionization potential of the BaOH radical from laser photoionization-molecular beam experiments and *ab initio* calculations

Maximiliano Rossa, Iván Cabanillas-Vidosa, Gustavo A. Pino, and Juan C. Ferrero^{a)}
INFIQC-Departamento de Fisicoquímica, Facultad de Ciencias Químicas, Universidad Nacional de Córdoba, X5000IUS Córdoba, Argentina and Centro Láser de Ciencias Moleculares, Universidad Nacional de Córdoba, X5000IUS Córdoba, Argentina

(Received 13 September 2011; accepted 17 January 2012; published online 10 February 2012)

The adiabatic ionization potential of the BaOH radical, as generated in a laser vaporization-supersonic expansion source has been determined by laser photoionization experiments to be (4.55 ± 0.03) eV. This value supports the three lowest out of seven previous experimental estimates, the former ranging from 4.35 to 4.62 eV. The present result is compared to *ab initio* calculations, as performed using both quantum chemistry at different levels of theory and density functional theory, and trying several effective core potentials and their accompanying basis sets for Ba. The most satisfactory agreement is obtained for either the adiabatic or vertical ionization potentials that derive from post-Hartree-Fock [MP2 and CCSD(T)] treatments of electron correlation, along with consideration of relativistic effects and extensive basis sets for Ba, in both BaOH and BaOH⁺. Such conclusions extend to the results of related calculations on the Ba–OH dissociation energies of BaOH and BaOH⁺, which were performed to help in calibrating the present computational study. Bonding in BaOH/BaOH⁺, as well as possible sources of discrepancy with previous experimental determinations of the BaOH adiabatic ionization potential are discussed. © 2012 American Institute of Physics. [doi:10.1063/1.3682283]

I. INTRODUCTION

The structure and bonding of alkaline-earth monohydroxides are being studied in increasing detail at present as experimental techniques improve and theoretical treatment of their electronic properties advances.^{1–5} The adiabatic ionization potential (IP_a) is a central quantity in this regard as providing information on how the electronic structure of the neutral differs from that of the cation. Along with the corresponding dissociation energies D_0 , such thermochemical properties are valuable for an accurate modeling of a number of gas-phase and cluster reactions involving the MOH and MOH⁺ (M = alkaline-earth metal atom) species.^{6–13}

The BaOH adiabatic ionization potential has thus far eluded definitive determination. Available experimental data, which rely on direct measurements of gas phase equilibria by spectroscopic and mass spectrometric detection in flames and by Knudsen cell and effusion mass spectrometry, range from 4.35 to 6 eV.^{14–18} In a review of earlier experimental work, the 1985 JANAF tables¹⁹ recommended a value of 5.09 eV, which significantly differs from the value of (4.77 ± 0.10) eV resulting from a further evaluation of experimental data.²⁰ The situation is also reflected in the BaOH IP_a values of (5 ± 1) eV, (5.3 ± 0.1) eV, and (4.4 ± 0.2) eV that are currently compiled in the NIST database,²¹ as adopted from the determinations in Refs. 14–16, respectively. The present work reports a new determination of $IP_a(\text{BaOH})$ (see Table I) through laser

photoionization experiments on the electronic ground-state BaOH radical, as generated in a laser vaporization-supersonic expansion source.²³ The use of a laser ionization source along with the rotational cooling of BaOH species attained in the supersonic expansion results in a lower uncertainty, by about one order of magnitude in $IP_a(\text{BaOH})$ with respect to previous estimates of this quantity.

The present and previous experimental values for $IP_a(\text{BaOH})$ are compared to the results of *ab initio* calculations, as performed using both quantum chemistry at different levels of theory and density functional theory, and trying several effective core potentials (and their accompanying basis sets) for Ba. Further calculations were performed on $D_0(\text{Ba–OH})$ and $D_0(\text{Ba}^+–\text{OH})$, and the results were compared with available data to help in calibrating the present computational study. Altogether, the present experimental and theoretical results are relevant in view of the large discrepancy spanning 0.9 eV between the three $IP_a(\text{BaOH})$ values, which are currently considered most reliable.²¹

II. EXPERIMENTAL

The BaOH radicals were generated in a homemade pickup, laser-vaporization source.²³ Barium vaporization was accomplished by mildly focusing the 1064 nm output of a pulsed Nd:YAG laser [Big Sky Laser-Quantel CFR 400, 5.5 ns full width at half maximum (FWHM), (1.4 ± 0.7) J/cm² laser fluence] onto the surface of a rotating pure Ba disk, which was placed 4 mm off-axis and 2 mm downstream from the nozzle of a pulsed solenoid valve (General Valve series

^{a)} Author to whom correspondence should be addressed. Electronic mail: jferrero@mail.fcq.unc.edu.ar. Tel.: +54 351 4334169/80. Fax: +54 351 4334188.

TABLE I. Experimental ionization potentials (eV) for the ground-state BaOH radical.

IP _a	Experimental technique	Method	Reference
4.5 ± 1	Knudsen cell mass spectrometry	Appearance potential	14
5.25 ± 0.1	Flame study using electrostatic probe detection	Second-law procedure	15
4.35 ± 0.3 ^a	Knudsen cell mass spectrometry	Appearance potential	16
6 ± 1	Effusion mass spectrometry	Appearance potential	17
5.09	...	Average of two separate measurements ^b	19
4.77 ± 0.10	...	Evaluation of experimental data	20
4.62 ± 0.30	Flame study using quadrupole mass spectrometric detection	Measurements of gas phase equilibria	18
4.55 ± 0.03	Supersonic-jet study using laser photoionization with TOF-MS detection	Numerical simulation of the PIE curve	This work

^aFrom the uncertainty of the appearance potential of BaOH reported in Ref. 16, it is apparent for the quoted value (± 0.2 eV) in the NIST Database (Ref. 21) to have a misprint.

^bReference 15 and flame study using microwave cavity resonance detection (Ref. 22).

9, 400 μm diameter). The laser-vaporized Ba species were perpendicularly entrained in a supersonic jet, as produced by expanding 2 bars of a He : H₂O (0.988 : 0.012) gas mixture through the pulsed valve.

The ensuing molecular beam, which contained BaOH products of the reaction between water and electronically excited Ba atoms, was collimated with a 4.0 mm diameter skimmer that was placed 6 cm downstream from the nozzle, before entering the ionization region of a differentially pumped, homemade Wiley-McLaren time-of-flight mass spectrometer (TOF-MS) with a mass resolution of $m/\Delta m = 355$.²⁴ The BaOH radicals were photoionized under single-photon ionization conditions at a total distance of 23 cm from the nozzle by either using a frequency-doubled dye laser (Lumonics HD500, 0.04 cm^{-1} bandwidth), operating on Rhodamines (R-610, R-590, and R-575, Exciton) and pumped by a Nd:YAG laser (Spectra-Physics INDI 40–10, 10 ns FWHM) at 532 nm, or the fourth harmonic (266 nm) of the latter. Photoions were detected on microchannel plates after mass separation through the TOF-MS (46 cm flight length). Mass spectra at various ionization photon energies in the range of 4.23–4.66 eV were recorded in a personal computer via fast digitizing oscilloscope (Tektronix TDS 3034B). A master pulse/delay generator running at a repetition rate of 10 Hz was used to control the timing sequence of the experiments.

The instability of the pick-up source due to shot-to-shot fluctuations avoided for the full frequency resolution of the dye laser to be exploited. Hence, its frequency-doubled output was varied in steps of 0.20–0.50 nm (0.003–0.008 eV) at wavelengths above 286 nm (4.34 eV), and an average of 3072 shots was used to generate the TOF spectra at each fixed wavelength. Further processing of the data, as described in Sec. IV led to the determination of the IP_a of BaOH.

Wavelength calibration of the fundamental output of the dye laser was performed by exciting both Ba atoms in the molecular beam and I₂ contained in a cell,²⁵ which resulted in an absolute resolution better than 0.005 nm within the photoionization wavelength range used.

The rotational temperature of BaOH radicals in the molecular beam was estimated from separate laser-

induced fluorescence (LIF) measurements on BaO molecules (IP_a = 6.91 eV) (Ref. 21), which are also present in the supersonic expansion presumably²³ as products of the reaction between water and ground-state Ba atoms. BaO molecules were probed 2 cm downstream from the faceplate of the pulsed valve within the source vacuum chamber by the fundamental output of the above-mentioned dye laser operating on F-548. LIF excitation spectra for the BaO ($A^1\Sigma^+$, $v' = 3$, $j' \leftarrow X^1\Sigma^+$, $v'' = 0$, j'') rovibrational band were obtained by detecting the total fluorescence onto a photomultiplier tube (Hamamatsu 1P28). Computer simulations of the spectra using relevant spectroscopic constants²⁶ yielded a best-fit BaO rotational temperature in the range of 50–75 K (see Figure 1), which is in line with related estimates on similar sources.^{1,27,28}

III. THEORETICAL METHODS

All of the *ab initio* calculations were carried out using the GAUSSIAN 03 suite of programs.²⁹ Following Bauschlicher *et al.*,^{30,31} extensive and flexible basis sets were used to describe the atoms in the BaOH/BaOH⁺ systems. The AUG-cc-pVTZ basis sets of Dunning and co-workers^{32,33} were used for the O and H atoms. A ten-valence electron effective core potential (ECP) treatment was instead employed for Ba. Particularly relevant to this study is the comparison of the performance of the relativistic effective core potential (RECP) earlier developed by Bauschlicher *et al.*,^{30,34} denoted as BJLMP/BLP hereafter, with that of the recently adjusted energy-consistent small-core RECP by Lim *et al.*,³⁵ denoted as LSS hereafter. These RECP's and their corresponding valence basis sets have been shown suitable to determine the geometries, harmonic frequencies, and IP_a's of small barium-containing species.^{30,31,36–39} Both the LANL2DZ RECP/valence basis set of Hay and Wadt⁴⁰ and the SDD quasirelativistic ECP/valence basis set of Kaupp *et al.*,⁴¹ as defined in the GAUSSIAN 03 package have also been evaluated for Ba.

The BaOH/BaOH⁺ geometries were optimized, and their vibrational frequencies were computed using the hybrid

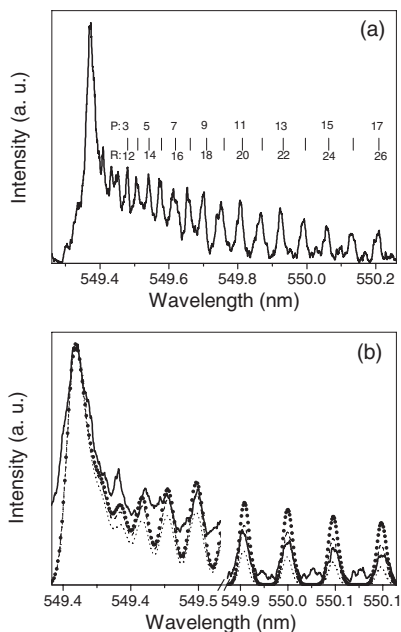


FIG. 1. (a) Typical LIF excitation spectrum showing rotational distribution of the ($A^1\Sigma^+$, $v' = 3 \leftarrow X^1\Sigma^+$, $v'' = 0$) band of BaO molecules present in the supersonic expansion. (b) Comparison of the experimental spectrum (—) with the computer simulations using ^{138}BaO rotational temperatures of 50 (\cdots), 75 ($-\cdot-\cdot-$), and 100 ($\bullet\cdots\bullet$) K. The background in the experimental spectrum, which is mostly observed in the range of 549.4–549.9 nm originates from overlapping, unresolved bands of lighter barium isotope-containing BaO species.

density functional B3LYP approach,^{42,43} the Hartree-Fock (HF) method, and the second-order Møller-Plesset (MP2) perturbation theory.⁴⁴ The resulting geometries were further used to carry out single-point energy calculations at the corresponding levels of theory. Single-point energies were also computed by the coupled cluster method with single and double excitations plus perturbative triples [CCSD(T)] (Ref. 45) based on the structures of B3LYP optimizations. All explicitly treated orbitals were correlated in the MP2 and CCSD(T) calculations. In all of the calculations unrestricted wave functions were used for BaOH.

At all levels of theory, both adiabatic and vertical ionization potentials of BaOH were evaluated as the difference in total energies, including a zero-point correction, between BaOH^+ and BaOH. As usual, the IP_a was referenced to the ionic and neutral ground state optimized geometries, while for the vertical ionization potential (IP_v) the ionic energy was taken at the optimized geometry of ground state BaOH.

Additional calculations were performed to evaluate the dissociation energies with respect to the potential minima of BaOH and BaOH^+ , $D_e(\text{BaOH})$ and $D_e(\text{BaOH}^+)$, respectively, through the formalism formerly used to treat the related MOH/MOH⁺ systems ($M = \text{Be, Mg, Ca, Sr}$, as well as Ba for MOH).^{30,31} Within this picture, bonding in the ground states of these radicals is predominantly of Ba^+-OH^- and $\text{Ba}^{+2}-\text{OH}^-$ character, and the corresponding wave functions are dominated by single configurations leading to the following relationship:

$$D_e(\text{BaOH}^{(n-1)+}) = E(\text{Ba}^{n+}) + E(\text{OH}^-) - E(\text{BaOH}^{(n-1)+}, r_e) - \text{IP}(\text{Ba}^{(n-1)+}) + \text{EA}(\text{OH}), \quad (1)$$

where $n = 1, 2$, $\text{IP}(\text{Ba})/\text{IP}(\text{Ba}^+)$ is the ionization potential of the Ba atom/cation, and $\text{EA}(\text{OH})$ is the electron affinity of OH. Both $D_e(\text{BaOH})$ and $D_e(\text{BaOH}^+)$ were determined by combining accurate experimental values for $\text{IP}(\text{Ba}) = 5.2117$ eV,⁴⁶ $\text{IP}(\text{Ba}^+) = 10.0038$ eV,⁴⁶ and $\text{EA}(\text{OH}) = 1.8277$ eV (Ref. 47) with single-point energy calculations for all of the relevant species at the HF, MP2, and CCSD(T) levels. In the CCSD(T) case, OH^- single-point energies were computed on the basis of B3LYP-optimized structures. In treating theoretically the BaOH radical, Bauschlicher *et al.* reported a self-consistent field value of 4.38 eV for $D_e(\text{BaOH})$.³⁰ While these authors used triple-zeta plus double polarization quality basis sets for the H and O atoms that differs from those used in this work, their $D_e(\text{BaOH})$ compares favorably with the HF value of 4.42 eV that derives here from the same RECP treatment, which provides confidence in the present calculations.

In all cases corrections for zero-point vibrational energy were applied to determine the relevant D_0 values from the calculated D_e 's. No corrections were applied for potential errors³⁰ in the present calculations as basis set superposition errors (BSSE) and basis set incompleteness. This is likely to result in lower bounds to D_0 as basis set incompleteness, which usually decreases the calculated D_0 values, is the largest potential error particularly at the post Hartree-Fock (post-HF) level.^{30,31} An estimate here of the BSSE for BaOH/BaOH⁺ via the counterpoise method⁴⁸ led to upper limits of 0.03 eV at the HF level, and of 0.16 eV at the MP2 and CCSD(T) levels for the results from the BJLMP/BLP and LSS RECP's, in accord with the values reported for MOH/MOH⁺ radicals.^{30,31}

For the sake of clarity, only the results of density functional B3LYP and post-Hartree-Fock [MP2 and CCSD(T)] treatments of electron correlation, using the BJLMP/BLP and LSS ECP's are presented here.⁴⁹

IV. RESULTS AND DISCUSSION

A substantial abundance of BaOH species has been observed in the beam produced by the present laser-vaporization source, which parallels the performance of pick-up source used in Ref. 27 under similar conditions. Mass resolution in the present TOF-MS is adequate to resolve the five most abundant isotopes of barium⁴⁶ in the signals of such species.²³ Figure 2(a) shows the photoionization efficiency (PIE) curve of BaOH, which results from numerically integrating the mass signal corresponding to $^{138}\text{BaOH}^+$ and normalizing the resulting area to the dye laser power. Since efficient frequency-doubling of the output of the available dye laser system is limited to wavelengths greater than 542 nm, no further tracing of the PIE curve above 4.58 eV could be made, except for a single measurement at 4.66 eV, i.e., the energy of the fourth-harmonic output (266 nm) of the pump laser.

Also shown in Fig. 2(a) is the most satisfactory numerical simulation of the PIE curve, as made under the assumption that only direct $\text{BaOH}^+ \leftarrow \text{BaOH}$ ionization occurs (i.e., neglecting the occurrence of autoionization) and considering that the photoionization probabilities of all relevant vibrational transitions are proportional to their Franck-Condon

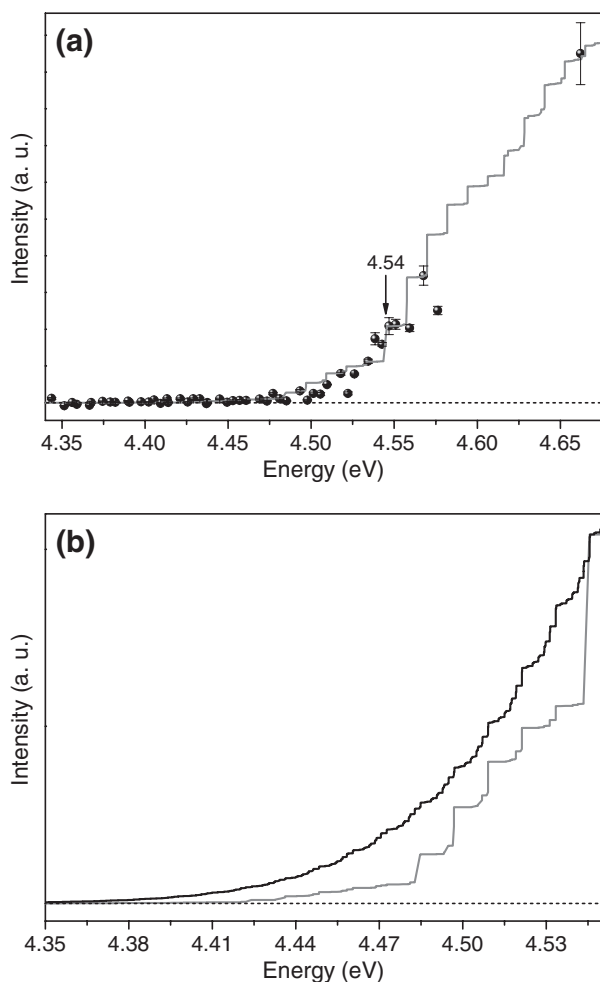


FIG. 2. (a) Comparison between the experimental photoionization efficiency curve (●) for the BaOH radical and the most satisfactory numerical simulation (grey line), as made by assuming that only direct ionization occurs, and taking the photoionization laser bandwidth, the rotational (75 K) and vibrational (500 K) temperatures of BaOH, and the relevant FCF into account. The best-fit value for $IP_a(\text{BaOH})$ is indicated by the vertical arrow. (b) Apparent ionization threshold behaviour of both the most satisfactory simulation in panel (a) (grey line) and a further numerical simulation (black line) using the same assumptions and parameters as to derive the $IP_a(\text{BaOH})$ while taking a BaOH vibrational temperature of 1829 K. The curves have been normalized to their corresponding plateaux at energies >5.5 eV. In panels (a) and (b), an extrapolation (---) of the baseline to the post-threshold portion of the PIE curve is also shown as a guide to the eye.

factors (FCF). This yields to best-fit values of 4.54 eV for the IP_a of BaOH and of 500 K for the BaOH vibrational temperature. The simulation procedure was as follows: On the basis of findings in the present calculations that the ground states of BaOH and BaOH⁺ have $2\Sigma^+$ and $1\Sigma^+$ symmetries, respectively, *P* and *R* rotational branches for all of the BaOH⁺($X^1\Sigma^+$; $\nu_1' = 0-6$, $\nu_2' = 0-6$, $\nu_3' = 0-3$) \leftarrow BaOH($X^2\Sigma^+$; $\nu_1'' = 0-6$, $\nu_2'' = 0-6$, $\nu_3'' = 0-3$) vibronic transitions were calculated using the spectral simulation program PGOPHER.⁵⁰ The rotational transitions were convoluted with a Gaussian line shape equal to the bandwidth of the dye laser (0.04 cm⁻¹), and a BaOH rotational temperature of 75 K (Sec. II) was employed in the simulations. For the simulation in Fig. 2, the required spectroscopic parameters for BaOH and BaOH⁺ were taken from the results of complementary theoretical calcula-

tions leading to the IP_a of BaOH, particularly from the present BJLMP/BLP RECP treatment at the B3LYP level. Table II lists the relevant, optimal geometric parameters, and the corresponding rotational constants and harmonic vibrational frequencies for the bending (ν_1) and stretching of Ba–O and O–H (ν_2 and ν_3 , respectively). At the energy resolution of the present PIE curve, though, it was found that the use of parameters arising from the SDD or LSS ECP treatments in combination with the B3LYP and MP2 levels of theory did not lead to noticeable differences regarding the results that derive from the preferred set of constants. After accounting for an assumed (statistical) population distribution of BaOH vibrational levels, as characterized by a vibrational temperature, and weighting the various rovibronic transitions on the corresponding FCF, integration over all transitions was performed to yield the PIE simulation.

In the above procedure, the band origin of the BaOH⁺($X^1\Sigma^+$; 0, 0, 0) \leftarrow BaOH($X^2\Sigma^+$; 0, 0, 0) vibrational transition corresponds to the IP_a of BaOH. Hence, the latter was derived from a simulation of the experimental PIE curve, using the IP_a and the vibrational temperature of BaOH as well as an overall scaling factor as fitting parameters. It follows from preliminary simulations that BaOH vibrational temperatures in the range of 450–550 K reproduce well both envelop and steepness of the experimental PIE curve in the recorded energy region including the single measurement at 4.66 eV. At any given BaOH vibrational temperature, though, relatively small changes in the corresponding input IP_a 's are found to affect markedly the agreement between simulation and experiment. For instance, a 0.01 eV decrease in BaOH IP_a at the preferred vibrational temperature of 500 K shifts the calculated PIE curve to the red along the energy scale, to the extent that the simulation increases faster than observed at all of the photoionization energies above 4.46 eV, while the opposite is true for a 0.01 eV increase in BaOH IP_a . Such findings imply that reliable values for the IP_a of BaOH, which are accurate to around 0.01 eV can be extracted from the fits here. Given the PIE curve in Fig. 2(a) where vibrational steps cannot be clearly discerned, the actual uncertainty of the present determination is estimated to be ± 0.03 eV. The latter considers three standard deviations of the fit, and includes estimates of the uncertainties arising mainly from the fact that the photoionization energy was varied in steps of less than 0.01 eV (Sec. II), and from signal-to-noise ratio.

The difference between the rotational temperature estimate of 50–75 K for BaOH (Sec. II) and the corresponding vibrational temperature of 500 K, as derived from the simulations above can be accounted for considering the classical situation in molecular beam experiments where rotational cooling is found to be more efficient than relaxation of vibrational degrees of freedom.⁵² Similar conclusions have been reported in a resonant two-photon ionization study on the vibrational structure of gas-phase Ba₂,²⁸ as generated using a pick-up source under similar conditions as here.

To the best-fit value for IP_a of 4.54 eV, 0.01 eV have been added in order to correct for the effect of the electric field ($E = 192$ V/cm) arising from the TOF-MS extraction plates,⁵³ which yields a final value of (4.55 ± 0.03) eV for the IP_a of BaOH. The present determination supports the three

TABLE II. Geometric parameters, harmonic vibrational frequencies, and rotational constants for the ground-state BaOH and BaOH⁺ radicals. Bond lengths r_e are in angstroms, bond angles \angle are in degrees, and vibrational frequencies ν_e , and rotational constants B_e are in cm⁻¹.

BaOH								
Method	Ba ECP/basis set	$r_e(\text{Ba-O})$	$r_e(\text{O-H})$	$\angle(\text{Ba-O-H})$	$\nu_e(\text{Ba-O-H}) - \pi$	$\nu_e(\text{Ba-O}) - \sigma$	$\nu_e(\text{O-H}) - \sigma$	B_e
B3LYP ^a	BJLMP/BLP	2.225	0.958	180.0	357.8	489.7	3896.0	0.2114
	LSS	2.223	0.958	180.0	339.6	493.0	3888.1	0.21219
MP2 ^a	BJLMP/BLP	2.222	0.957	180.0	415.3	492.1	3930.4	0.21207
	LSS	2.218	0.958	180.0	358.7	497.9	3902.7	0.21274
CISD ^b	BJLMP/BLP	2.234	502
Expt. ^c	n/a	2.201	0.923	180	341.6 ± 0.6	492.4 ± 0.8
BaOH ⁺								
Method	Ba ECP/Basis set	$r_e(\text{Ba-O})$	$r_e(\text{O-H})$	$\angle(\text{Ba-O-H})$	$\nu_e(\text{Ba-O-H}) - \pi$	$\nu_e(\text{Ba-O}) - \sigma$	$\nu_e(\text{O-H}) - \sigma$	B_e
B3LYP ^a	BJLMP/BLP	2.151	0.961	180.0	456.0	570.8	3865.5	0.22565
	LSS	2.148	0.961	180.0	436.9	574.1	3855.6	0.22623
MP2 ^a	BJLMP/BLP	2.145	0.959	180.0	503.2	571.3	3898.0	0.22678
	LSS	2.141	0.961	180.0	446.9	578.1	3864.8	0.22754

^aThis work.^bReference 30; unrestricted wave functions/Gaussian-type, triple-zeta plus double polarization quality basis sets of van Duijneveldt (as cited in Ref. 30) for the H and O atoms. $r_e(\text{O-H})$ and $\angle(\text{Ba-O-H})$ fixed at 0.9472 Å and 180°, respectively.^cLaser-induced fluorescence spectra in the gas phase (Ref. 51).

lowest previous estimates (Table I) while differing significantly from the value of (4.77 ± 0.10) eV derived from evaluation of experimental data.²⁰ The results from an early flame study [(5.25 ± 0.1) eV] (Ref. 15) and, particularly, a coarse effusion mass spectrometry determination [(6 ± 1) eV] (Ref. 17) seem too high for reasons that are not apparent.

Table III lists the calculated IP_a's and IP_v's of BaOH. Overall, the theoretical results provide support for the available experimental values below 5 eV (see Table I), which is in line with above conclusions from the comparison between the present and previous estimates of the BaOH IP_a. Particu-

larly for the BJLMP/BLP and LSS RECP's, treatment of electron correlation at the post-HF level leads generally to a good agreement with the experimental IP_a, which derives from this work. This conclusion holds irrespective of considering the theoretical IP_a or IP_v, given that at all levels of theory the IP_v-IP_a difference [(0.053 ± 0.007) eV; see Table III] is twice larger than the 0.03 eV uncertainty of the present determination.

The present theoretical results can also be used to unravelling possible sources of discrepancy with previous estimates for the IP_a of BaOH, particularly the mass

TABLE III. Theoretical ionization potentials (eV) for the ground-state BaOH radical, and dissociation energies D_0 (eV) for both ground-state BaOH and BaOH⁺ radicals.

Method	Ba ECP/Basis set	IP _a	IP _v	(Theoretical – Experimental ^a)	$D_0(\text{BaOH})$	$D_0(\text{BaOH}^+)$
				IP _a		
B3LYP ^a	BJLMP/BLP	4.672	4.717	0.122
	LSS	4.708	4.755	0.158
MP2 ^b	BJLMP/BLP	4.477	4.525	-0.073	4.39	4.94
	LSS	4.532	4.581	-0.018	4.36	5.00
CCSD(T) ^b	BJLMP/BLP	4.523	4.572	-0.027	4.45	4.97
	LSS	4.571	4.621	0.021	4.42	5.02
CISD ^c	BJLMP/BLP	4.6	...
Expt.	n/a	n/a	n/a	n/a	4.64 ^d , 4.94 ^e , 4.73 ± 0.13 ^f	5.35 ± 1 ^d , 5.5 ± 0.2 ^g
					4.64 ± 0.17 ^g , 4.57 ^h	4.70 ^h

^aExperimental IP_a = 4.55 eV (This work).^bThis work.^cReference 30; unrestricted wave functions/Gaussian-type, triple-zeta plus double polarization quality basis sets of van Duijneveldt (as cited in Ref. 30) for the H and O atoms. The $D_0(\text{BaOH})$ value incorporates corrections for errors in both computed Ba-OH bond length and RECP treatment of the Ba core electrons.^dKnudsen cell mass spectrometry (Ref. 14). The measured appearance potential and dissociation energy of BaOH were converted [through Eq. (2) below] to $D_0(\text{BaOH}^+)$ using IP(Ba) = 5.2117 eV (Ref. 46).^eAtomic absorption spectroscopy in flames (Ref. 54).^fFlame photometry (Ref. 55).^gKnudsen cell mass spectrometry (Ref. 16). From comparing the $D_0(\text{BaOH})$ values reported there both in kcal/mol (107) and in eV (4.55), it is apparent for the latter to have a misprint.^h1985 JANAF tables (Ref. 19).

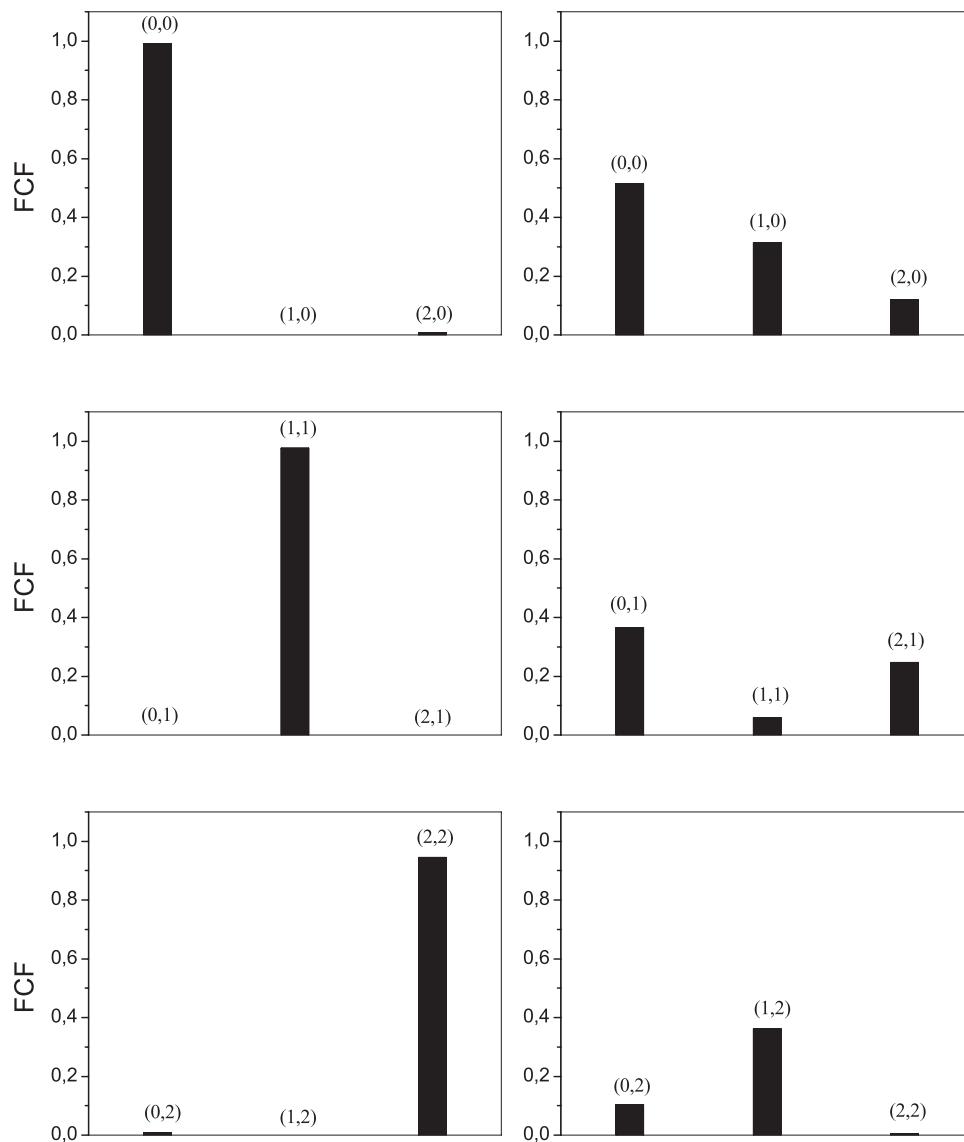


FIG. 3. Calculated Franck-Condon factors for the $\text{BaOH}^+(X^1\Sigma^+; v_1' = 0-2, 0, 0) \leftarrow \text{BaOH}(X^2\Sigma^+; v_1'' = 0-2, 0, 0)$ [left-hand column] and the $\text{BaOH}^+(X^1\Sigma^+; 0, v_2' = 0-2, 0) \leftarrow \text{BaOH}(X^2\Sigma^+; 0, v_2'' = 0-2, 0)$ [right-hand column] ionization process. The various (v', v'') pairs are indicated.

spectrometric determination in Ref. 16. In a 1990 evaluation of earlier experimental data, Belyaev *et al.*²⁰ compared their third-law calculations⁵⁶ for the IP_a 's of MOH (M = Ca, Sr, Ba) with the most accurate experimental estimates¹⁶ available from the corresponding appearance potentials (assuming them to be IP_a 's), and pointed out the discrepancy for the BaOH case [$\text{IP}_a = (4.85 \pm 0.18)$ eV and appearance potential = (4.35 ± 0.3) eV]. The difference was ascribed to the reduction in the appearance potential of BaOH, with respect to the corresponding IP_a , arising from vibrational excitation in the doubly degenerate bending mode of BaOH at the temperature of the experiment (1829 K).¹⁶ It was proposed that the distinct behavior of BaOH is due to a corresponding non-diagonal matrix of Franck-Condon factors for its bending. Here the FCF for both the $\text{BaOH}^+(X^1\Sigma^+; v_1' = 0-2, 0, 0) \leftarrow \text{BaOH}(X^2\Sigma^+; v_1'' = 0-2, 0, 0)$ and the $\text{BaOH}^+(X^1\Sigma^+; 0, v_2' = 0-2, 0) \leftarrow \text{BaOH}(X^2\Sigma^+; 0, v_2'' = 0-2, 0)$ processes were calculated using the spectroscopic parameters for BaOH/BaOH⁺, which derive from the B3LYP-BJLMP/BLP RECP theoretic-

cal treatment (Table II). The results are shown in Figure 3, from which it is apparent that the FCF matrix for the bending is nearly diagonal over several vibrational quantum numbers, at variance with the proposal in Ref. 20. Such an FCF envelope is to be expected from the finding in the present theoretical calculations of linear structures for both BaOH and BaOH⁺.⁴⁹ The FCF for Ba-O stretching is instead distributed evenly over several vibrational quantum numbers. The difference with the bending case can be traced to the variation in the $r_e(\text{Ba-O})$ and $v_e(\text{Ba-O})$ values, of $\sim 3\%$ and 16% , respectively, in going from BaOH to BaOH⁺, as found at all levels of theory and irrespective of the ECP used.⁴⁹ In this view, and considering that the magnitudes of $v_e(\text{Ba-O})$ and $v_e(\text{Ba-O-H})$ are similar to each other and much lower than that of $v_e(\text{O-H})$ (Table II), it is suggested here that BaOH excitation in the Ba-O stretching mode is more likely to explain the difference between the two above estimates for $\text{IP}_a(\text{BaOH})$ than BaOH bending excitation. This appears corroborated by numerical simulations of the PIE curve using the same

TABLE IV. Ionization potentials (eV) for the ground-state MOH (M = Be, Mg, Ca, Sr) radicals.

Species	Experimental IP _a (MOH) ^a	Theoretical IP _a (MOH)	[IP(M) – IP _a (MOH)] ^b
BeOH	9.0 ± 0.5 ^c	8.02 ^d	0.323
MgOH	7.5 ± 0.3 ^e	7.42 ^d	0.146
CaOH	5.6 ± 0.2 ^e , 5.9 ± 0.1 ^f , 6 ± 1 ^g	5.59 ^d	0.113–0.513
SrOH	5.1 ± 0.2 ^e , 5.6 ± 0.1 ^f	5.26 ^d	0.095–0.595
BaOH	4.55 ± 0.03 ^h	4.52–4.57 ⁱ	0.662

^aFor MOH (M = Mg, Ca, Sr), these values were taken from the NIST database (Ref. 21).

^bIP(M) (eV): Be (9.3227), Mg (7.6462), Ca (6.1132), Sr (5.6949), and Ba (5.2117), as taken from the NIST database (Ref. 46).

^cAppearance potential as reported in the 1985 JANAF tables (Ref. 19).

^dReference 31; CISD level using Gaussian-type orbital basis sets better than triple-zeta in the valence region, plus at least three sets of polarization functions (as cited in Ref. 30).

^eKnudsen cell mass spectrometry (Ref. 16).

^fReference 15.

^gEffusion mass spectrometry (Ref. 57).

^hThis work.

ⁱThis work: CCSD(T) level using BJLMP/BLP - LSS RECP theoretical treatments.

assumptions and parameters as to derive the IP_a(BaOH) while taking a BaOH vibrational temperature of 1829 K, which has clearly the effect of reducing the apparent ionization threshold below 4.36 eV [see Figure 2(b)].

It could be instructive to assess the present IP_a(BaOH) determination in the light of previous experimental values for IP_a of the lighter MOH (M = Be, Mg, Ca, Sr) species, which are listed in Table IV. The results of earlier calculations on the IP_a(MOH) at the CI(SD) level³¹ are also listed for comparison. For CaOH and SrOH, the discrepancy between the currently accepted determinations spans 0.4 and 0.5 eV, respectively. Notwithstanding, the agreement between experiment and theory is generally satisfactory except for BeOH where the single experimental value is about 1 eV larger. In the case of IP_a(BaOH), the fact that the present experimental and theoretical results altogether support the previous determinations below 5 eV would imply a narrowing, from about 1.7 eV to ~0.4 eV of the discrepancy between available experimental values (see Table I). The latter could be further narrowed to ~0.2 eV on the basis of the considerations made above on possible sources of errors in the most recent, mass spectrometric IP_a(BaOH) determination.¹⁶

The measured IP_a(BaOH) can be further used to substantiate the analogy with the isoelectronic alkaline earth monohalides,^{6,16} whereby bonding in ground state MOH and MOH⁺ is dominated by electrostatic forces due to their configurations M⁺–OH[–] and M²⁺–OH[–], respectively. Within this picture, electron removal in ground state MOH occurs from a nonbonding orbital located primarily on the metal atom and polarized away from the OH group. Notwithstanding, the ionization potentials of the MOH (M = Be, Mg, Ca, Sr, Ba) species are several eV's lower than the corresponding M⁺ → M²⁺ second ionization potentials.⁴⁶ In fact, it has been noted^{16,19,31} that the IP_a's of MOH species are similar to the ionization potentials of the corresponding metal atoms IP(M). This is illustrated in Table IV, where the IP(M)–IP_a(MOH)

difference has been listed. Clearly, these differences are small as compared to the IP(M)'s. Such observations are corroborated by the differences between the dissociation energies of MOH⁺ and MOH, which are related to the IP(M)–IP_a(MOH) difference by the expression,

$$D_0(M^+ - OH) - D_0(M - OH) = IP(M) - IP(MOH). \quad (2)$$

An experimental determination¹⁶ of D₀(BaOH) and D₀(BaOH⁺) leads to the value of (0.86 ± 0.37) eV for the D₀(BaOH⁺)–D₀(BaOH) difference, which is in good accord with the corresponding MP2 and CCSD(T) values that result from using either the BJLMP/BLP or LSS RECP's (Table III) and, more importantly, with the IP(Ba)–IP_a(BaOH) difference here (Table IV). This is also consistent with conclusions of previous studies at the CI(SD) level on D₀(M–OH)/D₀(M⁺–OH) for the MOH/MOH⁺ (M = Be, Mg, Ca, Sr) systems.^{30,31}

Altogether, the above observations can be rationalized by considering two contributing effects. In the first place, the electrostatic stabilization of the nearby OH[–] ion that nearly balances the energy required for ionization of the metal positive ion core.³¹ Second, the OH[–] ion electric field that distorts the nonbonding orbital, thus increasing (destabilizing) the unpaired electron's energy and decreasing the ionization potential.²⁰

V. CONCLUSIONS

A pick-up source has been applied to the determination in laser photoionization experiments of the adiabatic ionization potential of the BaOH radical yielding a new value of (4.55 ± 0.03) eV. The latter derives from numerical simulations of the PIE curve made by assuming that only direct ionization occurs (i.e., neglecting the occurrence of autoionization), and taking the photoionization laser bandwidth, the rotational and vibrational temperatures of BaOH, and the relevant FCF into account. The various spectroscopic parameters for BaOH/BaOH⁺, which result from complementary theoretical calculations, have been used in the simulations.

The present experimental value for IP_a(BaOH) is compared to the results of *ab initio* calculations, as performed using both quantum chemistry at different levels of theory and density functional theory, and trying several effective core potentials (and their accompanying basis sets) for Ba. The most satisfactory agreement is generally obtained for either the adiabatic or vertical ionization potentials that derive from post-Hartree-Fock [MP2 and CCSD(T)] treatments of electron correlation, along with consideration of relativistic effects and extensive basis sets for Ba, in both BaOH and BaOH⁺. Remarkably, the post-HF IP_a(BaOH) values for the BJLMP/BLP and LSS RECP theoretical treatments are within twice the 0.03 eV uncertainty of the present experimental determination (Table III). Such conclusions generally extend to the results of related calculations on the Ba–OH dissociation energies of BaOH and BaOH⁺, which were performed to help in

calibrating the present computational study. Overall, the evidence demonstrates that a quantitative description of the electronic and thermochemical properties of open-/closed-shell, heavy metal atom-containing radicals such as BaOH/BaOH⁺ can be achieved by an in-depth treatment of electron correlation and relativistic effects.

The present value for IP_a(BaOH) compares favorably with the three lowest out of seven previous experimental estimates, the former ranging from 4.35 to 4.62 eV. Further numerical simulations of the PIE using the same assumptions and parameters as to derive the IP_a(BaOH) while taking a BaOH vibrational temperature of 1829 K, provide further clues to possible sources of discrepancy with previous experimental determinations of IP_a(BaOH). In particular, it is suggested that the estimate of (4.35 ± 0.3) eV in Ref. 16 could be low as a result of BaOH vibrational excitation in both the Ba–O bending and stretching modes at the temperature of the experiment, which was not properly accounted for in the data deconvolution procedure for IP_a(BaOH).

Overall, the present experimental and theoretical results reinforce previous suggestions^{6,16,30,31,51,58} that the BaOH electronic structure and bonding can be derived from a diatomic molecule analogy (OH⁻ behaves like a pseudohalide), and that the BaOH/BaOH⁺ radicals have a highly ionic character.

ACKNOWLEDGMENTS

The authors are grateful to Philippe Maitre (Laboratoire de Chimie Physique, Université Paris-Sud XI, Orsay, France) for helpful comments and suggestions concerning the theoretical calculations, and to a referee for suggestions regarding treatment of the experimental data. Financial support from CONICET, FONCyT, SeCyT-UNC, and MinCyT Córdoba is also acknowledged. I.C.-V. and M.R. acknowledge doctoral and post-doctoral fellowships, respectively, from CONICET.

- ¹A. M. Ellis, *Int. Rev. Phys. Chem.* **20**, 551 (2001).
- ²M. C. Heaven, V. E. Bondybey, J. M. Merritt, and A. L. Kaledin, *Chem. Phys. Lett.* **506**, 1 (2011).
- ³M. B. Sullivan, M. A. Iron, P. C. Redfern, J. M. L. Martin, L. A. Curtiss, and L. Radom, *J. Phys. Chem. A* **107**, 5617 (2003).
- ⁴D. S. Ho, N. J. DeYonker, A. K. Wilson, and T. R. Cundari, *J. Phys. Chem. A* **110**, 9767 (2006).
- ⁵M. Vasiliiu, D. Feller, J. L. Gole, and D. A. Dixon, *J. Phys. Chem. A* **114**, 9349 (2010).
- ⁶C. G. James and T. M. Sugden, *Nature (London)* **175**, 333 (1955).
- ⁷C. Th. J. Alkemade, Tj. Hollander, W. Snelleman, and P. J. Th. Zeegers, *Metal Vapors in Flames* (Pergamon, Oxford, 1982).
- ⁸V. Blagojevic, A. Božović, G. Orlova, and D. K. Bohme, *J. Phys. Chem. A* **112**, 10141 (2008).
- ⁹R. K. Marcus, *J. Anal. At. Spectrom.* **19**, 591 (2004).
- ¹⁰M. Granet, A. Nonell, G. Favre, F. Chartier, H. Isnard, J. Moureau, C. Caussignac, and B. Tran, *Spectrochim. Acta., Part B* **63**, 1309 (2008).
- ¹¹A. T. Blades, P. Jayaweera, M. G. Ikonoumou, and P. Kebarle, *Int. J. Mass Spectrom. Ion Process.* **102**, 251 (1990).
- ¹²J. T. O'Brien, J. S. Prell, J. D. Steill, J. Oomens, and E. R. Williams, *J. Phys. Chem. A* **112**, 10823 (2008).
- ¹³A. L. Heaton, V. N. Bowman, J. Oomens, J. D. Steill, and P. B. Armentrout, *J. Phys. Chem. A* **113**, 5519 (2009).
- ¹⁴F. E. Stafford and J. Berkowitz, *J. Chem. Phys.* **40**, 2963 (1964).
- ¹⁵R. Kelly and P. J. Padley, *Trans. Faraday Soc.* **67**, 1384 (1971).
- ¹⁶E. Murad, *J. Chem. Phys.* **75**, 4080 (1981).
- ¹⁷M. Farber and R. D. Srivastava, *J. Chem. Phys.* **74**, 2160 (1981).
- ¹⁸J. M. Goodings, P. M. Patterson, and A. N. Hayhurst, *J. Chem. Soc., Faraday Trans.* **91**, 2257 (1995).
- ¹⁹M. W. Chase, Jr., C. A. Davies, J. R. Downey, Jr., D. J. Frurip, R. A. McDonald, and A. N. Syverud, *J. Phys. Chem. Ref. Data* **14**, 1 (1985).
- ²⁰V. N. Belyaev, I. S. Gotkis, N. L. Lebedeva, and K. S. Krasnov, *Russ. J. Phys. Chem.* **64**, 773 (1990).
- ²¹NIST Chemistry WebBook, see also <http://webbook.nist.gov>.
- ²²D. E. Jensen, *Combust. Flame* **12**, 261 (1968).
- ²³I. Cabanillas-Vidosa, M. Rossa, G. A. Pino, and J. C. Ferrero, *Phys. Chem. Chem. Phys.* **13**, 13387 (2011).
- ²⁴A. N. Oldani, M. Mobbili, E. Marceca, J. C. Ferrero, and G. A. Pino, *Chem. Phys. Lett.* **471**, 41 (2009).
- ²⁵S. Gerstenkorn and P. Luc, *Atlas du spectre d'absorption de la molécule de l'iode*, (14800-20000 cm⁻¹) (Editions du C.N.R.S., 1978).
- ²⁶N. Furio and J. G. Pruett, *J. Mol. Spectrosc.* **136**, 120 (1989).
- ²⁷S. J. Pooley, M. S. Beardah, and A. M. Ellis, *J. Electron. Spectrosc. Relat. Phenom.* **97**, 77 (1998).
- ²⁸M. A. Lebeault, J. Viallon, V. Boutou, and J. Chevalere, *J. Mol. Spectrosc.* **192**, 179 (1998).
- ²⁹M. J. Frisch, G. W. Trucks, H. B. Schlegel *et al.*, GAUSSIAN 03, Revision E.01, Gaussian, Inc., Pittsburgh, PA, 2004.
- ³⁰C. W. Bauschlicher, Jr., S. R. Langhoff, and H. Partridge, *J. Chem. Phys.* **84**, 901 (1986).
- ³¹H. Partridge, S. R. Langhoff, and C. W. Bauschlicher, Jr., *J. Chem. Phys.* **84**, 4489 (1986).
- ³²T. H. Dunning, Jr., *J. Chem. Phys.* **90**, 1007 (1989).
- ³³R. A. Kendall, T. H. Dunning, Jr., and R. J. Harrison, *J. Chem. Phys.* **96**, 6796 (1992).
- ³⁴C. W. Bauschlicher, Jr., R. L. Jaffe, S. R. Langhoff, F. G. Mascarello, and H. Partridge, *J. Phys. B* **18**, 2147 (1985).
- ³⁵I. S. Lim, H. Stoll, and P. Schwerdtfeger, *J. Chem. Phys.* **124**, 034107 (2006).
- ³⁶V. Mikhailov, M. D. Wheeler, and A. M. Ellis, *J. Phys. Chem. A* **107**, 4367 (2003).
- ³⁷I. S. Lim and Y. S. Lee, *J. Chem. Phys.* **126**, 104307 (2007).
- ³⁸S. Schäfer, M. Mehring, R. Schäfer, and P. Schwerdtfeger, *Phys. Rev. A* **76**, 052515 (2007).
- ³⁹J. Wang, D. Zhai, F. Guo, Y. Ouyang, Y. Du, and Y. Feng, *Theor. Chem. Acc.* **121**, 165 (2008).
- ⁴⁰P. J. Hay and W. R. Wadt, *J. Chem. Phys.* **82**, 299 (1985).
- ⁴¹M. Kaupp, P. v. R. Schleyer, H. Stoll, and H. Preuss, *J. Chem. Phys.* **94**, 1360 (1991).
- ⁴²A. D. Becke, *J. Chem. Phys.* **98**, 5648 (1993).
- ⁴³C. Lee, W. Yang, and R. G. Parr, *Phys. Rev. B* **37**, 785 (1988).
- ⁴⁴M. J. Frisch, M. Head-Gordon, and J. A. Pople, *Chem. Phys. Lett.* **166**, 281 (1990).
- ⁴⁵J. A. Pople, M. Head-Gordon, and K. Raghavachari, *J. Chem. Phys.* **87**, 5968 (1987).
- ⁴⁶NIST Physical Reference Data, see also <http://www.nist.gov/pml/data>.
- ⁴⁷J. R. Smith, J. B. Kim, W. C. Lineberger, *Phys. Rev. A* **55**, 2036 (1997).
- ⁴⁸S. F. Boys and F. Bernardi, *Mol. Phys.* **19**, 553 (1970).
- ⁴⁹See supplementary material at <http://dx.doi.org/10.1063/1.3682283> for a full list of theoretical results for BaOH/BaOH⁺, including those computed using the HF method and both SDD and LANL2DZ ECP's at different levels of theory.
- ⁵⁰PGOPHER, a program for simulating rotational structure, C. M. Western, University of Bristol, see also <http://pgopher.chm.bris.ac.uk>
- ⁵¹S. Kinsey-Nielsen, C. R. Brazier, and P. F. Bernath, *J. Chem. Phys.* **84**, 698 (1986).
- ⁵²*Atomic and Molecular Beam Methods*, edited by G. Scoles (Oxford University Press, New York, 1988).
- ⁵³R. Lindner, H. J. Dietrich, and K. Müller-Dethlefs, *Chem. Phys. Lett.* **228**, 417 (1994).
- ⁵⁴D. H. Cotton and D. R. Jenkins, *Trans. Faraday Soc.* **64**, 2988 (1968).
- ⁵⁵V. G. Ryabova, A. N. Khitrov, and L. V. Gurvich, *High Temp. (USSR)* **10**, 669 (1972).
- ⁵⁶V. N. Belyaev, N. L. Lebedeva, K. S. Krasnov, and L. V. Gurvich, *Matematicheskie Zadachi Khimicheskoi Termodinamiki (Mathematical Problems in Chemical Thermodynamics)* (Izd. Nauka, Novosibirsk, 1985), p. 227.
- ⁵⁷M. Farber, R. D. Srivastava, J. W. Moyer, and J. D. Leeper, *J. Chem. Soc. Faraday Trans. 2* **83**, 3229 (1987).
- ⁵⁸M. A. Anderson, M. D. Allen, W. L. Barclay, Jr., and L. M. Ziurys, *Chem. Phys. Lett.* **205**, 415 (1993).